

# pH-Mediated Stoichiometric Switching of Cucurbit[8]uril–Hoechst-33258 Complexes

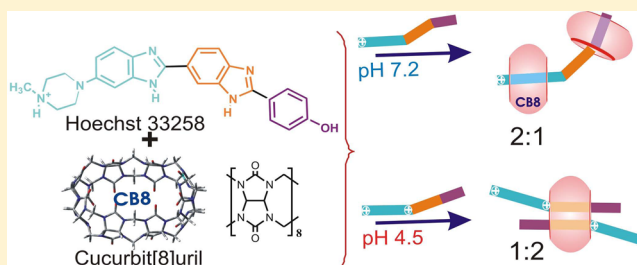
Nilotpal Barooah, Jyotirmayee Mohanty, and Achikanath C. Bhasikuttan\*

Radiation &amp; Photochemistry Division, Bhabha Atomic Research Centre, Mumbai 400 085, India

**S** Supporting Information

**ABSTRACT:** Stimuli-responsive molecular assemblies of potential drug/guest molecules through noncovalent host–guest interaction have been found very attractive in transporting and releasing the desired form on demand. In this article, the host–guest interaction of a drug, Hoechst-33258 (H33258), has been investigated in aqueous solutions in the presence of a macrocyclic host, namely, cucurbit[8]uril (CB8). The pH dependent structural conformations of H33258 are found to be decisive in determining the stoichiometry and geometry of the supramolecular assembly. Interaction of CB8

with the monocationic H33258 at pH 7.2 is very strong with an overall binding constant of the order of  $10^{11} \text{ M}^{-2}$ . The noncovalently stabilized assembly with 2:1 (CB8:H33258) stoichiometry brings out  $\sim 26$ -fold enhancement in the emission yield. On the other hand, the strong ion–dipole interactions provided by the dicationic dye at pH 4.5 support the CB8 to uptake two dicationic H33258 dyes in its cavity in a 1:2 stoichiometry ( $K_{(\text{pH } 4.5)} = (3.2 \pm 0.2) \times 10^{11} \text{ M}^{-2}$ ). In this case, the fluorescence displayed a quenching with a decrease in the emission yield from 0.4 to 0.2. The distinct pH-mediated stoichiometric switching of CB8–H33258 complexes and the contrasting fluorescence properties demonstrated here would find application in the field of biomolecular imaging and exchange of included guests for a selective drug transport/release.



## INTRODUCTION

Since the beginning of supramolecular chemistry, the molecular recognition events in synthetic or biomolecular systems revealing newer functional aspects have gained long-standing interests.<sup>1</sup> A simple host–guest system with well-defined stoichiometry behaves as a prototype system to study the interplay of various noncovalent interactions in the recognition event, structure–property relations, etc., and more importantly, the unique physicochemical advantages characteristic to such supramolecular systems.<sup>1–5</sup> Supramolecular approaches have proved to be exceedingly useful in applications like in optical sensors,<sup>6</sup> on–off switches,<sup>7</sup> logic gates,<sup>8</sup> photostabilization,<sup>9</sup> supramolecular catalysis,<sup>10,11</sup> drug delivery vehicles,<sup>12</sup> enzymatic assay,<sup>13</sup> nanocapsules,<sup>14</sup> supramolecular architectures,<sup>4,7</sup> and many other stimuli-responsive systems.<sup>15</sup> In this regard, a large number of supramolecular systems involving preorganized synthetic receptors such as crown ethers, calixarenes, cyclodextrins, and more recently cucurbiturils have been documented in the literature.<sup>1,5</sup> The cucurbit[*n*]uril (*n* = 5, 6, 7, 8, 10) family of macrocyclic receptors are the methylene-bridged cyclic oligomers obtained from the acid-catalyzed condensation of glycoluril with formaldehyde in which the number of glycoluril units determines the size of the cucurbituril cavity.<sup>3,5,16,17</sup> Cucurbit[*n*]uril (CB*n*) has two negatively polarized carbonyl-laced portals and a hydrophobic cavity. Due to its unique structural features and depending on the size and charge of the guests, CB*n* can interact through strong ion–dipole and/or hydrophobic interactions.<sup>3,16,17</sup> CB*n* have gained

much research interest in recent years because of their high binding affinity to a variety of guests such as metal ions, metal nanoparticles, cationic or neutral organic molecules, organometallics, and even protein residues.<sup>3,16–19</sup> Among the CB*n* homologues, because of its large cavity volume (479 Å<sup>3</sup>), CB8 has the unique ability to accommodate simultaneously two guest molecules in its cavity.<sup>7,20</sup> This has allowed the utility of CB8 as a dynamic interlink to assemble polymeric and multivalent systems.

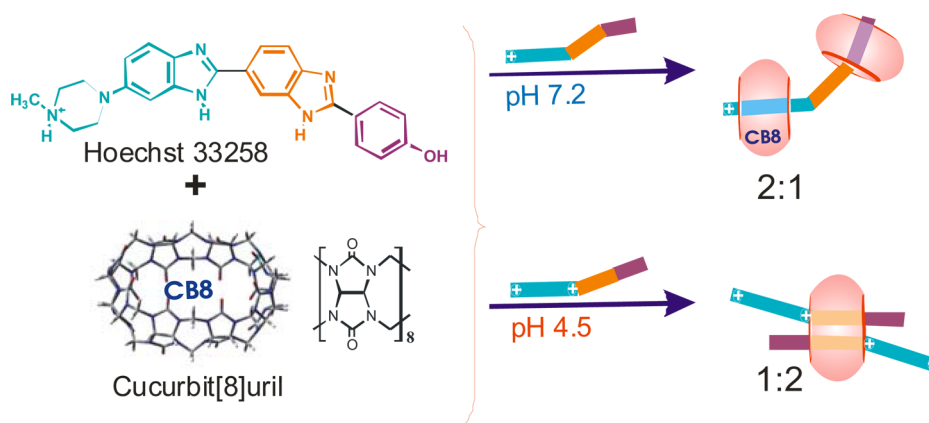
It was interesting to note that CB8 selectively forms ternary charge-transfer (CT) complex with an electron-deficient dicationic acceptor molecule such as methylviologen (MV<sup>2+</sup>) and an electron-rich donor such as 2,6-dihydroxynaphthalene in an aqueous media.<sup>21–24</sup> The unique ability of CB8 to form ternary host–guest complexes was recently utilized in the development of monodispersed microcapsules capable of on-demand release of encapsulated moieties under the influence of appropriate external stimuli.<sup>25,26</sup> In the same line, CB8-templated polymerization and supramolecular photocatalysis has been demonstrated by employing the dimer inclusion behavior of CB8 in aqueous medium.<sup>27,28</sup> For the past few years, our group has been investigating the various fronts of the host–guest chemistry of cucurbituril macrocycles especially, with fluorescent organic guest molecules which have led to the

Received: June 5, 2013

Revised: October 3, 2013

Published: October 3, 2013

**Scheme 1.** Structures of H33258 and CB8 Molecules and the Stoichiometric Arrangement Envisaged for Their Noncovalent Host–Guest Complexes Formed at the Specified pH Condition



demonstration of novel physicochemical aspects of the encapsulated moieties in aqueous medium.<sup>29–33</sup> Encapsulation of fluorogenic guests inside CB cavity bring about drastic modulation in their photophysical properties which are intrinsically related to their microenvironment, chemical identity (e.g., protonated/deprotonated forms) and stoichiometry (host:guest). Earlier, we have shown the excimer formation of thioflavin-T<sup>34</sup> and thiazole orange<sup>35</sup> dyes and the possibility of arranging a hetero dimer of neutral red and tryptophan guests<sup>36</sup> inside the CB8 cavity, bringing out their implications as “on–off” systems and for controlled release of drugs. In this context, there has been tremendous interest in exploring such stimuli-responsive cucurbituril assemblies of dyes/drugs, which have strong affinity toward biomolecules, such as DNAs, proteins, lipids, etc.<sup>37,38</sup>

Hoechst-33258 (H33258, Scheme 1) which belongs to the bisbenzimidazole class of dyes, has attracted immense research interest due to its antitumor<sup>39,40</sup> and antimicrobial<sup>41</sup> properties and some of its derivative are found to have potential as radioprotector.<sup>42,43</sup> Because of its double-strand DNA-binding affinity,<sup>44</sup> H33258 can affect transcription/translation and can block topoisomerase I as well as helicase activity.<sup>40,45,46</sup> Accordingly, this molecule can be very useful for the design of new drugs for gene regulation. On the other hand, H33258 exists in different conformations with respect to the pH of the media displaying diverse photophysical properties.<sup>47</sup> It has been widely accepted that the large fluorescence enhancement on binding to the minor grooves of DNA is due to the planar structure of the dye, which is largely devoid of the nonradiative channels.<sup>48,49</sup> Such structure–property relation can be easily introduced through macrocyclic encapsulation, especially by the CBs, which can preferentially stabilize different protolytic forms in distinct geometrical conformations.<sup>50</sup> In the presence of cucurbit[7]uril (CB7) macrocycle, the monocationic and the dicationic forms of H33258 interact in different ways forming 1:1 or 2:1 (host–guest) stoichiometric complexes, resulting in an upward  $pK_a$  shift in H33258.<sup>50</sup> In contrast to the case of CB7, its higher homologue, the CB8, interacts with H33258 quite differently, displaying contrasting fluorescence intensity changes with change in pH. In this article, we present a detailed photophysical evaluation of host–guest interaction of H33258 with CB8 macrocycle in aqueous medium at different solution pHs. The results demonstrate a pH-mediated stoichiometric switching between a 2:1 and 1:2 CB8–H33258 complexes, effected by the conformational distinction of the monocationic

and dicationic forms of H33258. The finding that the photophysical properties, the stoichiometry, and thus the release/activity of this DNA binder drug can be controlled by regulating the protolytic equilibrium in the presence of CB8 provides a valuable strategy for the uptake of selective guest pairs for targeted delivery.

## ■ EXPERIMENTAL SECTION

Hoechst-33258·3HCl was obtained from Sigma-Aldrich, USA, and CB8 was obtained from Aldrich. Nanopure water (conductivity of 0.06 mS cm<sup>−1</sup>), obtained from a Millipore Gradient Elix-3/A10 system, was used to prepare the sample solutions. <sup>1</sup>H NMR spectra were recorded on a Bruker Avance WB 500 MHz spectrometer at TIFR, India. For <sup>1</sup>H NMR spectra at different pD, NaOD (20% in D<sub>2</sub>O) and DCl (32% in D<sub>2</sub>O) were used to adjust the pD. Absorption spectra were recorded with a Shimadzu 160 A UV–vis spectrophotometer (Kyoto, Japan). Steady-state fluorescence spectra were recorded using a Hitachi F-4500 spectrofluorimeter (Tokyo, Japan). The samples were excited close to the isosbestic points, unless specified otherwise, and the changes in the absorbance if any at the excitation wavelength were normalized and the fluorescence intensities were corrected accordingly. The fluorescence quantum yield was estimated by comparing the integrated fluorescence intensity (corrected spectrum) of the H33258 system with that of a standard, Coumarin 152 ( $\phi_f$  acetonitrile 0.22), as described elsewhere.<sup>51</sup> The time-resolved (TR) fluorescence measurements were carried out using a time-correlated single-photon-counting (TCSPC) spectrometer (Horiba Jobin Yvon IBH, UK). In the present work, a 374 nm diode laser (fwhm 100 ps, 1 MHz repetition rate) was used for sample excitation and an MCP-PMT was used for fluorescence detection. A deconvolution procedure was used to analyze the observed decays.<sup>51</sup> The fluorescence decays  $I(t)$  were analyzed using a multiexponential function as

$$I(t) = \sum B_i \exp(-t/\tau_i) \quad (1)$$

where  $B_i$  and  $\tau_i$  are the pre-exponential factor and the fluorescence lifetime, respectively, for the  $i$ th component of the fluorescence decay. For anisotropy measurements, samples were excited with a vertically polarized excitation beam and the vertically and horizontally polarized fluorescence decays were collected with a large spectral bandwidth of ~32 nm. By use of

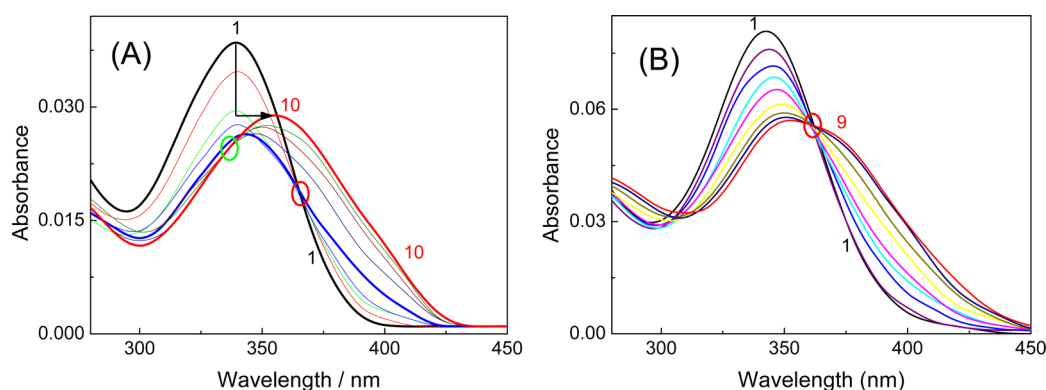


**Figure 1.** (A) Absorption spectra of H33258 (0.9  $\mu\text{M}$ ) recorded in 5 mM Tris-HCl buffer at pH 7 with [CB8]/ $\mu\text{M}$  0 (1); 0.2 (2); 0.4 (3); 0.7 (4); 1.3 (5); 2.5 (6); 4.0 (7); 5.0 (8); 7.0 (9); 9 (10). (B) Absorption spectra of H33258 (1.5  $\mu\text{M}$ ) recorded in 5 mM sodium acetate buffer at pH 4.5 with [CB8]/ $\mu\text{M}$  0 (1); 0.2 (2); 0.9 (3); 1.4 (4); 1.8 (5); 2.7 (6); 3.7 (7); 5.0 (8); 9 (9).

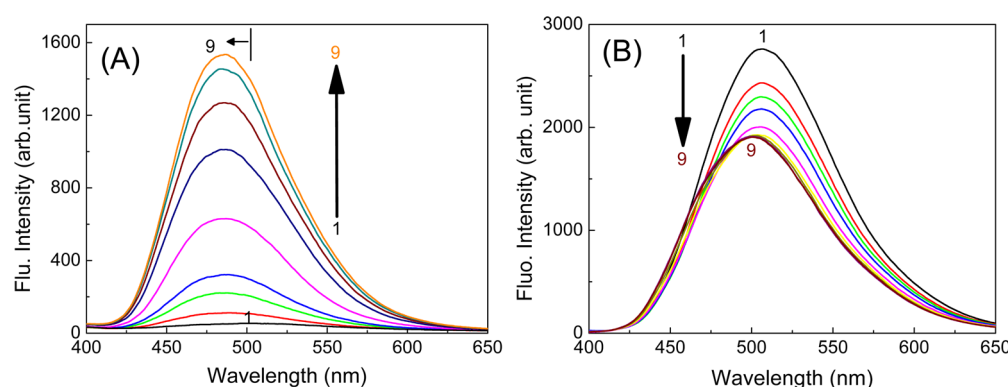


**Figure 2.** (A) Steady-state fluorescence spectra of H33258 (1  $\mu\text{M}$ ) recorded in 5 mM Tris.HCl buffer at pH 7 on excitation at 353 nm with [CB8]/ $\mu\text{M}$  0 (1); 0.2 (2); 0.4 (3); 0.7 (4); 1.3 (5); 2.5 (6); 4.0 (7); 5.9 (8); 9 (9). (B) Emission spectra of H33258 (1.5  $\mu\text{M}$ ) recorded in 5 mM sodium acetate buffer at pH 4.5 on excitation at 365 nm with [CB8]/ $\mu\text{M}$  0 (1); 0.2 (2); 0.4 (3); 0.9 (4); 1.8 (5); 2.7 (6); 3.7 (7); 6.8 (8); 9 (9). The arrows follow the change in the emission maximum with [CB8].

these polarized fluorescence decays, the anisotropy decay function,  $r(t)$ , was constructed as follows<sup>51</sup>

$$r(t) = \frac{I_V(t) - GI_H(t)}{I_V(t) + 2GI_H(t)} \quad (2)$$

where  $I_V(t)$  and  $I_H(t)$  are the vertically and horizontally polarized decays, respectively, and  $G$  is the correction factor for the polarization bias of the detection setup. The  $G$  factor was determined independently by using a horizontally polarized excitation beam and measuring the two perpendicularly polarized fluorescence decays. From the fluorescence anisotropy decays the rotational correlation time ( $\tau_r$ ), and hence the rotational diffusion coefficients ( $D_r$ ), can be arrived at using the Stokes–Einstein relationship<sup>52</sup>

$$\tau_r = 1/(6D_r), \quad \text{where } D_r = \frac{RT}{6V\eta} \quad (3)$$

where  $V$  is the hydrodynamic molecular volume of the complex (approximated as a rigid sphere)  $\eta$  is the viscosity of the medium, and  $T$  is the absolute temperature. Computational studies were performed with the Gaussian suite of packages.<sup>53</sup>

## RESULTS AND DISCUSSION

**Absorption and Emission Studies.** The photophysical properties of H33258 largely depend on the solution pH due to its different protolytic forms.<sup>54</sup> In aqueous solution at pH 7.2,

H33258 exists as monocationic displaying characteristic absorption maximum at 338 nm (Figure 1A). On titration with CB8, the absorption spectrum of H33258 (0.9  $\mu\text{M}$ , 5 mM Tris-HCl) displayed a hypochromic change with an isosbestic point at 365 nm as shown in Figure 1. When the CB8 concentration was increased further (up to  $\sim 9 \mu\text{M}$ ), the absorption displayed a bathochromic shift  $\sim 17$  nm to register the new absorption maximum at 355 nm. On the other hand, similar titration measurements at pH 4.5 (5 mM acetate buffer), where the dye exists in its dicationic form, displayed a different course. As presented in Figure 1B, at pH 4.5, H33258 displayed an absorption maximum at 343 nm and the addition of CB8 resulted in a hypochromic change with appearance of a prominent shoulder band at  $\sim 375$  nm and a neat isosbestic point at 362 nm.

These distinct absorption changes in the presence of CB8 at different pH conditions not only depict the complexation induced changes in the absorption characteristics of H33258 but also point to a probable change in the CB8-H33258 structure and stoichiometry. As discussed,<sup>54</sup> since H33258 exists as monocationic and dicationic at pH 7.2 and 4.5, respectively, it is likely that their molecular interaction with CB8 host would also be quite different affecting the spectral features.

To examine the emission behavior of H33258 in the above solutions, steady-state fluorescence spectra were recorded, in both the absence and presence of CB8. At pH 7.2, the dye

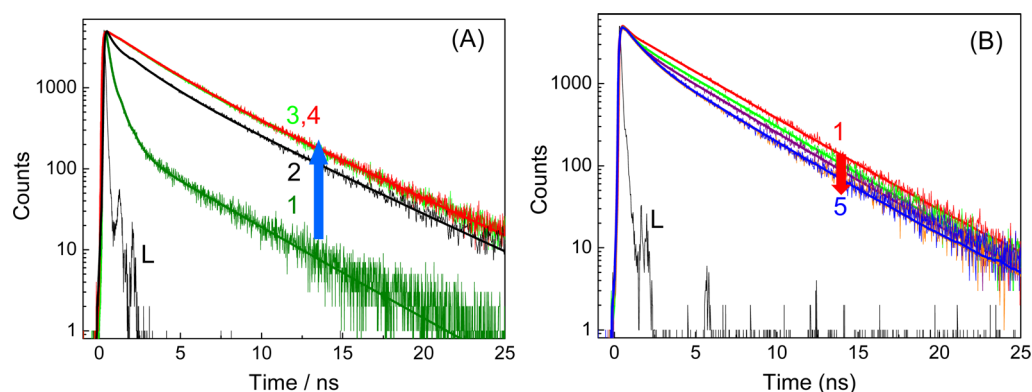


**Figure 3.** (A) Fluorescence decay traces of H33258 (1  $\mu\text{M}$ ) recorded at 500 nm in 5 mM Tris-HCl buffer at pH 7.2 with [CB8]/ $\mu\text{M}$  0 (1); 0.3 (2); 1.4 (3); 9 (4). (B) Decay traces of H33258 (2  $\mu\text{M}$ ) recorded at 500 nm in 5 mM sodium acetate buffer at pH 4.5 with [CB8]/ $\mu\text{M}$  0 (1); 0.9 (2); 1.8 (3); 6.7 (4); 9 (5).  $\lambda_{\text{ex}}$  = 374 nm. “L” represents excitation lamp profile.

**Table 1. Fluorescence Lifetime and Anisotropy Parameters Derived from Their Decay Trace Analysis at the Respective Solution Conditions<sup>a</sup>**

H33258	CB8	lifetime				$\chi^2$	anisotropy $\tau_r$ (ns)
		$\tau_1$ (ns) $a_1$ (%)	$\tau_2$ (ns) $a_2$ (%)	$\tau_3$ (ns) $a_3$ (%)			
1 $\mu\text{M}$ at pH 7.2 (5 mM Tris-HCl)	0	0.15 (31)	0.58 (42)	3.80 (27)	1.03	$0.32 \pm 0.04$	
	0.3 $\mu\text{M}$	0.21 (9)	1.91 (28)	4.60 (63)	1.10		
	1.4 $\mu\text{M}$	—	2.35 (35)	4.74 (65)	1.08		
	9 $\mu\text{M}$	—	2.37 (35)	4.74 (65)	1.05		
2 $\mu\text{M}$ at pH 4.5 (5 mM acetate buffer)	0	—	0.26 (3)	3.80 (97)	1.03	$0.37 \pm 0.02$	
	1 $\mu\text{M}$	—	0.49 (9)	3.74 (91)	1.13		
	3.7 $\mu\text{M}$	—	0.87 (22)	3.70 (78)	1.11		
	9 $\mu\text{M}$	—	0.95 (26)	3.70 (74)	1.14		

<sup>a</sup> $a_i$  is the pre-exponential factor for the respective lifetime components.

H33258 (0.9  $\mu\text{M}$ , 5 mM Tris-HCl) displayed a very weak emission spectrum centered at 510 nm (Figure 2A). Upon gradual addition of CB8 (up to  $\sim 9 \mu\text{M}$ ) the emission displayed a dramatic enhancement in intensity with a concomitant hypsochromic shift ( $\sim 20$  nm) of the emission maximum to 485 nm as shown in Figure 2A. At neutral pH, the monocationic H33258 is weakly fluorescent ( $\phi_f$  0.015) due to excited-state energy dissipation by the fast torsional motion in the excited state with respect to the single bond joining the two benzimidazole units.<sup>50,54</sup> Inclusion of H33258 in the rigid hydrophobic cavity of CB8 consequently restricts this fast torsional motion and also provides a hydrophobic micro-environment for the guest. These two factors lead to the fluorescence enhancement and also to the blue shift of the emission profile in the presence of CB8. Note that the quantum yield of emission for the CB8–H33258 complex increases to 0.4, indicating an overall 26-fold enhancement in emission yield in the presence of CB8 at pH 7.2.

On the other hand, H33258 shows quite contrasting emission features in the presence of CB8 at pH 4.5. At this pH, H33258 predominantly exists in the dicationic form with the protonation of the benzimidazole attached to the piperazinyl unit. The dicationic H33258 (2  $\mu\text{M}$ , pH 4.5 (5 mM acetate buffer) displays strong emission ( $\phi_f$  = 0.40), having emission maximum at 505 nm.<sup>54</sup> Interestingly, as shown in Figure 2B, addition of CB8 (up to  $\sim 5 \mu\text{M}$ ) resulted in quenching of the H33258 emission with a slight blue shift of the emission maximum by 5 nm. No further quenching was observed with increase in concentration of CB8 beyond 9  $\mu\text{M}$ .

At this solution condition the quantum yield is estimated to be 0.2.

These contrasting emission behaviors of H33258 in the presence of CB8 at pH 7.2 and 4.5 are intriguing, since at both these pH conditions, the CB7 analogue having smaller cavity dimension displayed significant enhancement in the emission intensity.<sup>50</sup> In recent reports on different chromophoric dyes such as thioflavin T (ThT),<sup>34</sup> thiazole orange (TO),<sup>35</sup> and neutral red (NR),<sup>36</sup> we have shown that CB8 can encapsulate more than one guest, thereby stabilizing homo/hetero guest pairs in the cavity. However, depending on the guest characteristics, the CB8–dye system provided emission quenching (in case of neutral red dye) whereas the CB8–ThT/TO systems presented strong emission bands due to an excimer formation. In the present case of H33258, the above observations point to the prospect of CB8 as a template for more than one H33258, having strong dependence on the solution pH. From the structural point of view, it is reasonable to visualize that the interaction of puckered monocationic form at neutral pH and the more planar dicationic form of H33258 at pH 4.5 with the macrocyclic receptor CB8 would be different and can support distinct host–guest complexes of different stoichiometries.

**Time-Resolved Fluorescence Measurements.** As discussed, in aqueous solution the emission intensity of H33258 at pH 7 is quenched dramatically ( $\phi_f$  = 0.015), whereas at pH 4.5 the fluorescence yield increases to 0.4.<sup>54</sup> It is known that two major processes are involved in the deactivation of the excited state of H33258, which are very sensitive to the solution conditions like solvent, pH, temperature, etc. As shown in



Figure 3A at pH 7.2, H33258 displayed a multiexponential decay kinetics having major decay components in the range of 100–400 ps and a slower component in the range of 3.5–4 ns (Table 1). However, at pH 4.5 (Figure 3B), the decay becomes nearly single exponential with 3.8 ns as the major lifetime component (97%), while the short component ( $\sim 0.26$  ns) contributes merely 3% (Table 1). In H33258, there are two benzimidazole units, one with a piperazine unit and the other with a phenol unit. At pH 4.5, the piperazine-attached benzimidazole is protonated, which allows certain degree of charge transfer (CT) from the protonated benzimidazole to the phenol-substituted benzimidazole, leading to a more planar structure, believed to be having lifetime in the range of 3.5–4 ns.<sup>48,49,54</sup> On the other hand, at pH 7.2, both the benzimidazole units are unprotonated and are in nonplanar conformation.<sup>49,54</sup> In this case, an internal conversion via intramolecular ring rotation becomes the dominant relaxation channel (100–340 ps, 70–80%) for the excited state and hence the population of the longer lived CT state (3.5–4 ns) becomes less probable. Depending on the pH and the dye concentration, the fluorescence decay of H33258 has been found to be biexponential<sup>49,55</sup> while a few other reports present them as triexponential.<sup>54,56</sup> It has been noted that the faster decay component largely depends on the protonation state of H33258, solvent viscosity, hydrogen bonding, and other interactions which affect its structural orientation.<sup>48–50,54</sup>

In the presence of cucurbituril hosts, the fast torsional relaxation is expected to get reduced on forming inclusion complexes. As seen from Figure 3A and Table 1 at pH 7.2, with the addition of CB8, the initial faster decay component seen in H33258 becomes slower and at  $\sim 1.4$   $\mu\text{M}$  of CB8 ( $\sim 1$  equiv of the H33258 concentration), the fluorescence decay best fitted to a biexponential kinetics having two time constants, 2.37 ns (35%) and 4.74 ns (65%). The decay profile remains unchanged with further increase in the CB8 concentration up to  $\sim 9$   $\mu\text{M}$ , suggesting no further structural/stoichiometric changes, like that observed in the case of the H33258–CB7 system at similar pH conditions.<sup>50</sup> Due to the intrinsic affinity of the cucurbituril macrocycles toward cationic guests and considering the molecular structure of the H33258 dye, inclusion complex formation through encapsulation of both the benzimidazole moieties is quite likely, which would retard the intramolecular torsional movement of H33258. As discussed above, at pH 7.2 both the benzimidazole units in H33258 are unprotonated and they exist both in nonplanar and more planar conformations, having significant differences in their excited-state lifetimes (Table 1). In the presence of CB8, it is quite expected that the proposed 2:1 (CB8:H33258) complex would stabilize these conformers independently, displaying distinct lifetime values. On this basis, we attribute the 2.37 ns and  $\sim 4.74$  ns lifetime components evaluated at pH 7.2 in the presence of  $\sim 9$   $\mu\text{M}$  of CB8 (at saturation condition) to different planar/nonplanar conformers feasible for the dye in the 2:1 complex.

On the other hand, H33258 at pH 4.5 ( $\sim 2$   $\mu\text{M}$ , 5 mM acetate buffer) displayed 3.8 ns decay component as the major deactivation pathway. Addition of CB8 to this solution resulted in the appearance of a faster decay component of  $\sim 0.9$  ns, which became prominent with  $\sim 26\%$  contribution in presence of 9  $\mu\text{M}$  of CB8 (Figure 3B, Table 1). This decrease in the average lifetime of H33258 in the presence of CB8 at pH 4.5 is appropriately seen as partial fluorescence intensity quenching in the steady-state measurement also. Since, the monocationic and

the dicationic H33258 differ in charge and structural conformations, the absorption and fluorescence spectral changes observed here would certainly point to different modes of binding in these two cases. As compared to the monocationic form, the dicationic H33258 is more planar with increased positive charge density and it is quite rational that two such guest dyes bind to the CB8 host by inclusion through either portals of the CB8 cavity. Such a guest dimer arrangement within the CB8 cavity can provide strong  $\pi$ -stacking interaction among the guests in the excited state, thus introducing a faster relaxation pathway and hence the emission quenching.

**Time-Resolved Fluorescence Anisotropy Decay of CB8–H33258 Complexes.** Time-resolved fluorescence anisotropy measurements can provide information regarding the rotational diffusion time of a fluorescent species, which could be correlated to the effective hydrodynamic size of the complex. The anisotropy decays,  $r(t)$ , recorded in the absence and presence of CB8 at the specified pH conditions, clearly presented large differences in the decay profiles (Figure 4),

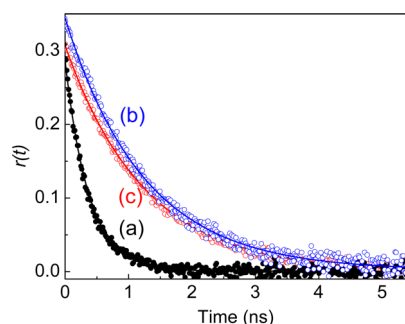


**Figure 4.** Anisotropy decay traces monitored at 500 nm for H33258 in 5 mM sodium acetate buffer at pH 4.5 in the absence (a) and in the presence of 9  $\mu\text{M}$  CB8 (b). Trace (c) represents the decay at pH 7.2 (5 mM Tris-HCl) in the presence of 5  $\mu\text{M}$  CB8. The solid lines represent the fitted exponential curves.  $\lambda_{\text{ex}} = 374$  nm.

pointing to an increase in the hydrodynamic molecular volume of H33258 in the presence of CB8. For the dye alone at pH 4.5, the anisotropy decay fits to a single-exponential kinetics with a time constant ( $\tau_r$ ) of  $0.37 \pm 0.02$  ns (Figure 4a) whereas at pH 7.2 the faster  $\tau_r$  decay is evaluated to be  $0.32 \pm 0.04$  ns. However, in the presence of CB8, the  $\tau_r$  gets significantly increased to  $1.30 \pm 0.01$  ns (Figure 4b) and  $1.20 \pm 0.01$  ns (Figure 4c), respectively at pH 7.2 and 4.5, conceding an increase in hydrodynamic molecular volume due to the complex formation. However, a demarcation of the structural/stoichiometric differences among these complexes is cumbersome as both the structures may have effectively similar hydrodynamic size.

**Determination of Stoichiometry and Geometry.** From the photophysical changes observed for H33258 in the presence of CB8 at pH 7.2 and 4.5, it is clear that interaction of H33258 with CB8 leads to distinct host–guest stoichiometric complexes specific to the solution pH, which imply the interactions of the monocationic and the dicationic forms of the dye with the CB8 host. The stoichiometric compositions were estimated by Job's continuous variation method in aqueous solutions at the preset pHs.<sup>50</sup> The plot at pH 7.2 (Figure 5A, 1) displayed an absorbance maximum at 0.65 mole fraction of CB8 ( $\eta_{\text{CB8}}$ ), validating a 2:1 (CB8:H33258) stoichiometry for the complex. However, with the dicationic dye at pH 4.5, the Job's

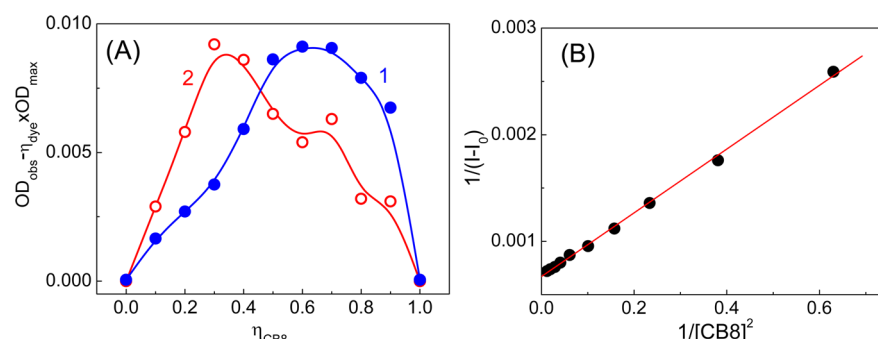


**Figure 5.** (A) Job's plot generated by continuous variation of the mole fraction of H33258 and CB8 from aqueous solutions at pH 7.2 (1) and at pH 4.5 (2). The total concentration was kept at 10  $\mu\text{M}$  and the absorption changes were monitored at 370 nm in both the cases. (B) Plot of the reciprocal of the fluorescence intensity changes at 500 nm for 2  $\mu\text{M}$  H33258 in  $\text{H}_2\text{O}$  versus  $1/[\text{CB8}]^2$ ,  $\lambda_{\text{ex}} = 353 \text{ nm}$ .

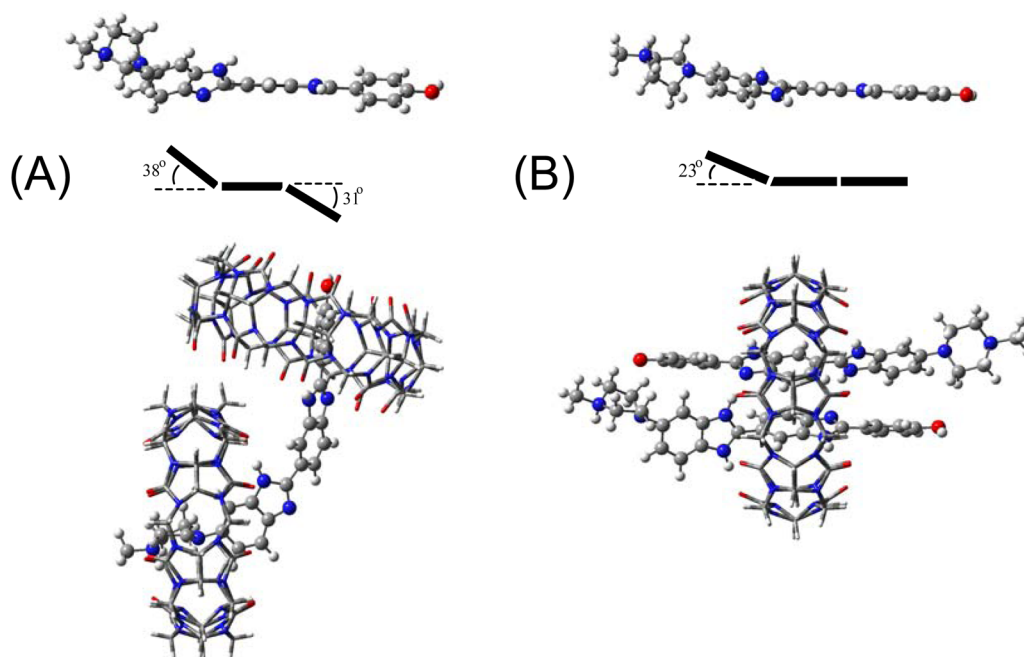


**Figure 6.** Geometry-optimized structures of H33258 and the CB8–H33258 complexes where H33258 is monocationic (A) and dicationic (B).

plot displayed a maximum at 0.33 mole fraction of CB8 (Figure 5A, 2), which suits a 1:2 (CB8:H33258) composition. It may be noted here that indication of an intermediate 1:1 composition is not possible from these measurements.

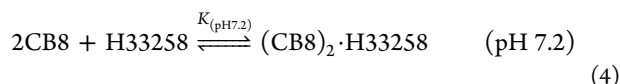
The proposed stoichiometric compositions and the geometrical arrangements for the monocationic and the dicationic dyes were further explored by the geometry optimization studies using semiempirical PM3 (MM) level calculation with Gaussian package.<sup>53</sup> As shown in Figure 6, depending on the charge and planarity of the monocationic and dicationic forms of H33258, 2:1 (−55 kcal/mol) and 1:2 (−16.5 kcal/mol) stoichiometries were found to be energetically favorable with the respective forms. For the monocationic form (Figure 6A), one of the most stable configurations is provided by the structure, which accommodates the CB8 moiety at the piperazine end as well at the phenol end, providing maximum ion dipole and hydrogen-bonding interaction among the host–guest and also among the CB8 hosts. It is interesting to see that the puckered monocationic H33258 prefers an unusually bend structure, quite distinct from the more planar structure observed for the same guest with CB7 host.<sup>50</sup> Here, the carbonyl portals of one of the CB8 moieties find several

protons from the other CB8 moiety in the hydrogen-bonding distance of  $\sim 2.5 \text{ \AA}$ . The probability of such nonplanar conformer is readily seen in the excited-state lifetime values discussed before. However, in the case of the dicationic H33258, the two protonated nitrogen centers in the H33258 get stabilized by the large negative charge density at the CB8 portals and allow  $\pi$ -stacking interaction among the two H33258s placed inside the CB8 cavity as in Figure 5B. It may be mentioned here that since the geometry optimizations were done without the consideration of any solvent and other medium parameters, these models provide only a qualitative picture of the structures in the ground state.  $^1\text{H}$  NMR spectroscopic measurements could not be practically utilized for the evaluation of the binding sites and stoichiometry, due to very low solubility of the CB8 ( $\sim 90 \mu\text{M}$  in the absence of salts or acid). However, qualitative differences in the aromatic region ( $\delta$  8.5–6) of H33258  $^1\text{H}$  NMR peaks in the presence of CB8 at the two pH conditions were seen, supporting the above contentions (Figure S1 in the Supporting Information (SI)).

The possibility of a change in the protolytic equilibria due to complexation has also been considered. The  $\text{pK}_a$  measurement in the presence of CB8 (Figure S2 in the SI) did not display

any credible  $pK_a$  shift assignable to any of the photophysical changes observed here. Thus, the differential uptake of the protonated forms of H33258 by the CB8, both in stoichiometry and geometry, is established in relation to the solution pH and a schematic visualization of the complexation at the two pH conditions are displayed in Scheme 1. Such pH-mediated stoichiometric switching of CB8–H33258 complexation equilibrium opens up several tunable supramolecular applications. Since H33258 is a well-known DNA binder and a drug, controlled partition of the desired protolytic form using the biocompatible CB macrocycles<sup>57</sup> would be interesting. It may be also possible to selectively replace the homo dimer with a hetero dimer complex of better stability and applicability with biomolecules, and this is currently being pursued.

**Binding Constants.** Having established the stoichiometric arrangements of the CB8–H33258 complexes at pH 7.2 and 4.5, the following host–guest equilibria are proposed at the respective pHs. Though we observed changes in the absorption spectra indicating a two-stage complexation at pH 7.2 (Figure 1A), other experimental data suggest that these interactions are essentially simultaneous. Hence, for simplicity, we consider only the 2:1 equilibrium at pH 7.2 and the binding constant value has been evaluated from a modified Benesi–Hildebrand plot of the emission intensity at 500 nm versus the CB8 concentration. As per the equilibrium

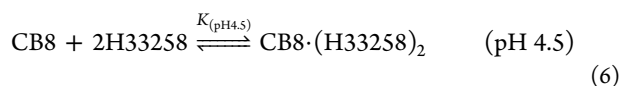


the overall binding constant ( $K_{(\text{pH } 7.2)}$ ) for the reaction can be obtained from the modified Benesi–Hildebrand relation<sup>58</sup>

$$\frac{1}{I - I_0} = \frac{1}{(I_\infty - I_0)K_1[\text{CB8}]^2} + \frac{1}{I_\infty - I_0} \quad (5)$$

where  $I_0$  and  $I$  are the fluorescence intensities of H33258 in the absence and presence of CB8, respectively, and  $I_\infty$  is the fluorescence intensity of H33258 when all molecules are complexed by the CB8. From the linear plot obtained for  $1/(I - I_0)$  versus  $1/[\text{CB8}]^2$  (Figure 5B),  $K_{(\text{pH } 7.2)}$  is estimated to be  $(2.1 \pm 0.2) \times 10^{11} \text{ M}^{-2}$ .

On the other hand at pH 4.5, considering a 1:2 host–guest stoichiometry, the complexation equilibrium can be expressed as



and observed binding constant ( $K_{(\text{pH } 4.5)}$ ) can be expressed as<sup>36</sup>

$$K_{(\text{pH} 4.5)} = \frac{[\text{CB8} \cdot (\text{H33258})_2]}{[\text{H33258}]^2 [\text{CB8}]} \quad (7)$$

If  $a$  is the concentration of the H33258 in the absence of CB8 host and  $b$  is the concentration of the CB8 with respect to the 50% of the total change in fluorescence intensity, then

$$K_{(\text{pH} 4.5)} = \frac{\left(\frac{a}{2 \times 2}\right)}{\left\{\left(\frac{a}{2}\right)^2 \times b\right\}} \quad (8)$$

Following the above equation, the estimated overall binding constant  $K_{(\text{pH } 4.5)}$  for the equilibrium (6) at pH 4.5 is  $(3.2 \pm 0.2) \times 10^{11} \text{ M}^{-2}$ .

## CONCLUSION

In this study, we have demonstrated a pH-mediated stoichiometric switching of cucurbit[8]uril–Hoechst-33258 complexes, revealing distinct photophysical properties. The well-known DNA binder drug Hoechst-33258 displays very strong pH-dependent photophysical changes due to the geometrical differences in their protonated states. With the monocationic H33258 at pH 7.2, the CB8 interaction is very strong and the noncovalently stabilized assembly brings out a 2:1 (CB8:H33258) stoichiometry with  $\sim 26$ -fold enhancement in the emission yield, suitable for biomolecular imaging. On the other hand, the strong ion–dipole interaction provided by the more planar dicationic H33258 at pH 4.5 supports the CB8 to accommodate two dicationic H33258 in its cavity in a 1:2 stoichiometry. Due to this, the emission yield decreases from 0.4 to 0.2. Since the stoichiometry and thus the release/activity of drug can be controlled by regulating the protolytic equilibrium, the macromolecular encapsulation of selective guest pairs of H33258 in the CB8 cavity provides design input for host–guest-based drug delivery systems and their applications.

## ASSOCIATED CONTENT

### Supporting Information

Additional figures and discussions. This material is available free of charge via the Internet at <http://pubs.acs.org>.

## AUTHOR INFORMATION

### Corresponding Author

\*E-mail: [bkac@barc.gov.in](mailto:bkac@barc.gov.in).

### Notes

The authors declare no competing financial interest.

## ACKNOWLEDGMENTS

We gratefully acknowledge the support from the host institute, Bhabha Atomic Research Centre, for this research work.

## REFERENCES

- (1) Lehn, J.-M. Supramolecular chemistry: Receptors, catalysts, and carriers. *Science* **1985**, 227, 849–856.
- (2) Schneider, H.-J. Binding mechanisms in supramolecular complexes. *Angew. Chem., Int. Ed.* **2009**, 48, 3924–3977.
- (3) Bhasikuttan, A. C.; Pal, H.; Mohanty, J. Cucurbit[n]uril based supramolecular assemblies: tunable physico-chemical properties and their prospects. *Chem. Commun.* **2011**, 47, 9959–9971.
- (4) Frampton, M. J.; Anderson, H. L. Insulated molecular wires. *Angew. Chem., Int. Ed.* **2007**, 46, 1028–1064.
- (5) Dsouza, R. N.; Pischel, U.; Nau, W. M. Fluorescent dyes and their supramolecular host–guest complexes with macrocycles in aqueous solution. *Chem. Rev.* **2011**, 111, 7941–7980.
- (6) Wang, R.; Yuan, L.; Macartney, D. H. A green to blue fluorescence switch of protonated 2-aminoanthracene upon inclusion in cucurbit[7]uril. *Chem. Commun.* **2005**, 5867–5869.
- (7) Ko, Y. H.; Kim, E.; Hwang, I.; Kim, K. Supramolecular assemblies built with host-stabilized charge-transfer interactions. *Chem. Commun.* **2007**, 1305–1315.
- (8) Pischel, U.; Uzunova, V. D.; Remon, P.; Nau, W. M. Supramolecular logic with macrocyclic input and competitive reset. *Chem. Commun.* **2010**, 46, 2635–2637.
- (9) Mohanty, J.; Nau, W. M. Ultraprecise rhodamine with cucurbituril. *Angew. Chem., Int. Ed.* **2005**, 44, 3750–3754.
- (10) Pluth, M. D.; Bergman, R. G.; Raymond, K. N. Acid catalysis in basic solution: A supramolecular host promotes orthoformate hydrolysis. *Science* **2007**, 316, 85–88.



- (11) Singleton, M. L.; Reibenspies, J. H.; Darensbourg, M. Y. A Cyclodextrin Host/Guest Approach to a Hydrogenase Active Site Biomimetic Cavity. *J. Am. Chem. Soc.* **2010**, *132*, 8870–8871.
- (12) Jeon, Y. J.; Kim, S.-Y.; Ko, Y. H.; Sakamoto, S.; Yamaguchi, K.; Kim, K. Novel molecular drug carrier: encapsulation of oxaliplatin in cucurbit[7]uril and its effects on stability and reactivity of the drug. *Org. Biomol. Chem.* **2005**, *3*, 2122–2125.
- (13) Ghale, G.; Ramalingam, V.; Urbach, A. R.; Nau, W. M. Determining protease substrate selectivity and inhibition by label-free supramolecular tandem enzyme assays. *J. Am. Chem. Soc.* **2011**, *133*, 7528–7535.
- (14) Dutta Choudhury, S.; Mohanty, J.; Pal, H.; Bhasikuttan, A. C. Cooperative metal Ion binding to a cucurbit[7]uril-thioflavin T Complex: Demonstration of a stimulus-responsive fluorescent supramolecular capsule. *J. Am. Chem. Soc.* **2010**, *132*, 1395–1401.
- (15) Angelos, S.; Yang, Y.-W.; Patel, K.; Stoddart, J. F.; Zin, J. I. pH-responsive supramolecular nanovalves based on cucurbit[6]uril pseudorotaxanes. *Angew. Chem., Int. Ed.* **2008**, *47*, 2222–2226.
- (16) Lee, J. W.; Samal, S.; Selvapalam, N.; Kim, H.-J.; Kim, K. Cucurbituril homologues and derivatives: new opportunities in supramolecular chemistry. *Acc. Chem. Res.* **2003**, *36*, 621–30.
- (17) Lagona, J.; Mukhopadhyay, P.; Chakrabarti, S.; Isaacs, L. The cucurbit[n]uril family. *Angew. Chem., Int. Ed.* **2005**, *44*, 4844–4870.
- (18) Barooah, N.; Bhasikuttan, A. C.; Sudarsan, V.; Dutta Choudhury, S.; Pal, H.; Mohanty, J. Surface functionalized silver nanoparticle conjugates: demonstration of uptake and release of a phototherapeutic porphyrin dye. *Chem. Commun.* **2011**, *47*, 9182–9184.
- (19) Heitmann, L. M.; Taylor, A. B.; Hart, P. J.; Urbach, A. R. Sequence-specific recognition and cooperative dimerization of N-terminal aromatic peptides in aqueous solution by a synthetic host. *J. Am. Chem. Soc.* **2006**, *128*, 12574–12581.
- (20) Ling, Y.; Wang, W.; Kaifer, A. E. A new cucurbit[8]uril-based fluorescent receptor for indole derivatives. *Chem. Commun.* **2007**, 610–612.
- (21) Kim, H.-J.; Heo, J.; Jeon, W. S.; Lee, E.; Kim, J.; Sakamoto, S.; Yamaguchi, K.; Kim, K. Selective inclusion of a hetero-guest pair in a molecular host: Formation of stable charge-transfer complexes in cucurbit[8]uril. *Angew. Chem., Int. Ed.* **2001**, *40*, 1526–1529.
- (22) Rauwald, U.; Biedermann, F.; Deroo, S.; Robinson, C. V.; Scherman, O. A. Correlating solution binding and ESI-MS stabilities by incorporating solvation effects in a confined cucurbit[8]uril system. *J. Phys. Chem. B* **2010**, *114*, 8606–8615.
- (23) Ko, Y.; Kim, K.; Kang, J.; Chun, H.; Lee, J.; Sakamoto, S.; Yamaguchi, K.; Fetting, J.; Kim, K. Designed self-assembly of molecular necklaces using host-stabilized charge-transfer interactions. *J. Am. Chem. Soc.* **2004**, *126*, 1932–1933.
- (24) Kim, K.; Kim, D.; Lee, J. W.; Ko, Y. H.; Kim, K. Growth of poly(pseudorotaxane) on gold using host-stabilized charge-transfer interaction. *Chem. Commun.* **2004**, 848–849.
- (25) Biedermann, F.; Scherman, O. A. Cucurbit[8]uril Mediated Donor–Acceptor Ternary Complexes: A Model System for Studying Charge-Transfer Interactions. *J. Phys. Chem. B* **2012**, *116* (9), 2842–2849.
- (26) Zhang, J.; Coulston, R. J.; Jones, S. T.; Geng, J.; Scherman, O. A.; Abell, C. One-Step Fabrication of Supramolecular Microcapsules from Microfluidic Droplets. *Science* **2012**, *335*, 690–694.
- (27) Liu, Y.; Fang, R.; Tan, X.; Wang, Z.; Zhang, X. Supramolecular polymerization at low monomer concentrations: Enhancing intermolecular interactions and suppressing cyclization by rational molecular design. *Chem.—Eur. J.* **2012**, *18*, 15650–15654.
- (28) Barooah, N.; Pemberton, B. C.; Sivaguru, J. Manipulating photochemical reactivity of coumarins within cucurbituril nanocavities. *J. Org. Lett.* **2008**, *10*, 3339–3342.
- (29) Dutta Choudhury, S.; Mohanty, J.; Upadhyaya, H. P.; Bhasikuttan, A. C.; Pal, H. Photophysical studies on the noncovalent interaction of thioflavin T with cucurbit[n]uril macrocycles. *J. Phys. Chem. B* **2009**, *113*, 1891–1898.
- (30) Dutta Choudhury, S.; Mohanty, J.; Bhasikuttan, A. C.; Pal, H. A fluorescence perspective on the differential interaction of riboflavin and flavin adenine dinucleotide with cucurbit[7]uril. *J. Phys. Chem. B* **2010**, *114*, 10717–10727.
- (31) Mohanty, J.; Jagtap, K.; Ray, A. K.; Nau, W. M.; Pal, H. Molecular encapsulation of fluorescent dyes affords efficient narrow-band dye laser operation in water. *ChemPhysChem* **2010**, *11*, 3333–3338.
- (32) Barooah, N.; Mohanty, J.; Pal, H.; Bhasikuttan, A. C. Stimulus-responsive supramolecular pKa tuning of cucurbit[7]uril encapsulated coumarin 6 dye. *J. Phys. Chem. B* **2012**, *116*, 3683–3689.
- (33) Barooah, N.; Mohanty, J.; Pal, H.; Bhasikuttan, A. C. Non-covalent interactions of coumarin dyes with cucurbit[7]uril macrocycle: modulation of ICT to TICT state conversion. *Org. Biomol. Chem.* **2012**, *10*, S055–S062.
- (34) Mohanty, J.; Dutta Choudhury, S.; Upadhyaya, H. P.; Bhasikuttan, A. C.; Pal, H. Control of the supramolecular excimer formation of thioflavin T within a cucurbit[8]uril host: A fluorescence on/off mechanism. *Chem.—Eur. J.* **2009**, *15*, S215–S219.
- (35) Mohanty, J.; Thakur, N.; Dutta Choudhury, S.; Barooah, N.; Pal, H.; Bhasikuttan, A. C. Recognition-mediated light-up of thiazole orange with cucurbit[8]uril: Exchange and release by chemical stimuli. *J. Phys. Chem. B* **2012**, *116*, 130–135.
- (36) Shaikh, M.; Dutta Choudhury, S.; Mohanty, J.; Bhasikuttan, A. C.; Pal, H. Contrasting guest binding interaction of cucurbit[7–8]urils with neutral red dye: controlled exchange of multiple guests. *Phys. Chem. Chem. Phys.* **2010**, *12*, 7050–7055.
- (37) Shaikh, M.; Mohanty, J.; Bhasikuttan, A. C.; Uzunova, V. D.; Nau, W. M.; Pal, H. Salt-induced guest relocation from a macrocyclic cavity into a biomolecular pocket: interplay between cucurbit[7]uril and albumin. *Chem. Commun.* **2008**, 3681–3683.
- (38) Bhasikuttan, A. C.; Mohanty, J.; Nau, W. M.; Pal, H. Efficient fluorescence enhancement and cooperative binding of an organic dye in a supra-biomolecular host–protein assembly. *Angew. Chem., Int. Ed.* **2007**, *46*, 4120–4122.
- (39) Chen, A. Y.; Yu, C.; Gatto, B.; Liu, L. F. DNA minor groove-binding ligands: A different class of mammalian DNA topoisomerase I inhibitors. *Proc. Natl. Acad. Sci. U.S.A.* **1993**, *90*, 8131–8135.
- (40) Soderlind, K.-J.; Gorodetsky, B.; Singh, A. K.; Bachur, N. B.; Miller, G. G.; Lown, J. W. Bis-benzimidazole anticancer agents: targeting human tumor helicases. *Anti-Cancer Drug Des.* **1999**, *14*, 19–36.
- (41) Disney, M. D.; Stephenson, R.; Wright, T. W.; Haidaris, C. G.; Turner, D. H.; Gigliotti, F. Activity of hoechst 33258 against pneumocystis carinii f. sp. muris, candida albicans, and candida dubliniensis. *Antimicrob. Agents Chemother.* **2005**, *49*, 1326–1330.
- (42) Lyubimova, N. V.; Coultas, P. G.; Yuen, K.; Martin, R. F. In vivo radioprotection of mouse brain endothelial cells by Hoechst 33342. *Br. J. Radiol.* **2001**, *74*, 77–82.
- (43) Ojha, H.; Murari, B. M.; Anand, S.; Hassan, M. I.; Ahmad, F.; Choudhury, N. K. Interaction of DNA minor groove binder Hoechst 33258 with bovine serum albumin. *Chem. Pharm. Bull.* **2009**, *57*, 481–486.
- (44) Latt, S. A. Microfluorometric detection of deoxyribonucleic acid replication in human metaphase chromosomes. *Proc. Natl. Acad. Sci. U.S.A.* **1973**, *70*, 3395–3399.
- (45) Bailly, C. Topoisomerase I poisons and suppressors as anticancer drugs. *Curr. Med. Chem.* **2000**, *7*, 39–58.
- (46) Steinmetzer, K.; Reinert, K.-E. Multimode interaction of Hoechst 33258 with eukaryotic DNA; quantitative analysis of the DNA conformational changes. *J. Biomol. Struct. Dyn.* **1998**, *15*, 779–791.
- (47) Barooah, N.; Mohanty, J.; Pal, H.; Sarkar, S. K.; Mukherjee, T.; Bhasikuttan, A. C. pH and temperature dependent relaxation dynamics of Hoechst-33258: a time resolved fluorescence study. *Photochem. Photobiol. Sci.* **2010**, *10*, 35–41.
- (48) Guan, Y.; Shi, R.; Li, X.; Zhao, M.; Li, Y. Multiple binding modes for dicationic hoechst 33258 to DNA. *J. Phys. Chem. B* **2007**, *111*, 7336–7344.



- (49) Adhikary, A.; Buschmann, V.; Muller, C.; Sauer, M. Ensemble and single-molecule fluorescence spectroscopic study of the binding modes of the bis-benzimidazole derivative hoechst 33258 with DNA. *Nucleic Acids Res.* **2003**, *31*, 2178–2186.
- (50) Barooah, N.; Mohanty, J.; Pal, H.; Bhasikuttan, A. C. Supramolecular assembly of hoechst-33258 with cucurbit[7]uril macrocycle. *Phys. Chem. Chem. Phys.* **2011**, *13*, 13117–13126.
- (51) Lakowicz, J. R. *Principles of Fluorescence Spectroscopy*; Springer: New York: 2006.
- (52) Valeur, B., Ed. *Molecular Fluorescence Principles and Applications*. Wiley-VCH: Weinheim, Germany, 2002.
- (53) Frisch, M. J. et al. *GAUSSIAN 92, Revision E.1*; Gaussian Inc.: Pittsburgh, PA, 1992.
- (54) Barooah, N.; Mohanty, J.; Pal, H.; Sarkar, S. K.; Mukherjee, T.; Bhasikuttan, A. C. pH and temperature dependent relaxation dynamics of Hoechst-33258: a time resolved fluorescence study. *Photochem. Photobiol. Sci.* **2010**, *10*, 35–41.
- (55) Cosa, G.; Focsaneanu, K. S.; McLean, J. R.; McNamee, J. P.; Scaiano, J. C. Photophysical properties of fluorescent DNA-dyes bound to single- and double-stranded DNA in aqueous buffered solution. *Photochem. Photobiol.* **2001**, *73*, 585–599.
- (56) Hard, T.; Fan, P.; Kearns, D. R. A fluorescence study of the binding of Hoechst 33258 and DAPI to the halogenated DNAs. *Photochem. Photobiol.* **1990**, *51*, 77–86.
- (57) Uzunova, V. D.; Cullinane, C.; Brix, K.; Nau, W. M.; Day, A. I. Toxicity of cucurbit[7]uril and cucurbit[8]uril: an exploratory in vitro and in vivo study. *Org. Biomol. Chem.* **2010**, *8*, 2037–2042.
- (58) Mohanty, J.; Bhasikuttan, A. C.; Dutta Choudhury, S.; Pal, H. Noncovalent interaction of 5,10,15,20-tetrakis(4-N-methylpyridyl)-porphyrin with cucurbit[7]uril: A supramolecular architecture. *J. Phys. Chem. B* **2008**, *112*, 10782–10785.